Research Square

Preprints are preliminary reports that have not undergone peer review.
They should not be considered conclusive, used to inform clinical practice,
or referenced by the media as validated information.

Detection and Characterization of Latency Stage of EBV and Histopathological Analysis of Prostatic Adenocarcinoma Tissues

Khalid Ahmed
Aga Khan University
Alisalman Sheikh
Aga Khan University
Saira Fatima
Aga Khan University Hospital
Ghulam Haider
Aga Khan University
Kulsoom Ghias
Aga Khan University
Farhat Abbas
Aga Khan University
Nouman Mughal
Aga Khan University
Syed Hani Abidi (m.haniabidi@gmail.com)
Aga Khan University

Research Article

Keywords: Prostate carcinoma, prostatic adenocarcinoma, benign prostatic hyperplasia, BPH, EBV, EBV latency profile, Gleason score, tumor grade

Posted Date: February 11th, 2022

DOI: https://doi.org/10.21203/rs.3.rs-1301965/v1

License: This work is licensed under a Creative Commons Attribution 4.0 International License. Read Full License

Abstract

Introduction: The pathophysiology of prostate cancer involves both genetic and acquired factors, including pathogens, such as viruses. A limited number of studies have shown the presence of Epstein-Barr virus (EBV) in prostate cancer tissues. However, there is a dearth of data exploring EBV latency profile in prostate cancer, and the relationship of EBV with histopathological features of prostate cancer. In this study, prostate cancer and benign prostatic hyperplasia (BPH) samples were screened for the presence of EBV, followed by the characterization of the EBV latency profile and analysis of histopathological parameters in EBV-positive and EBV-negative groups.

Material & Methods: A conventional PCR strategy was employed using virus-specific primers to screen EBV in 99 formalin-fixed paraffin-embedded (FFPE) prostate cancer and 33 BPH samples received for histopathological analysis during the years 2019-2020. Subsequently, cDNA samples were used in a qPCR array to analyze the expression of EBV latency-associated genes to map the latency profile EBV maintains in the samples. Finally, statistical analyses were performed to determine the correlation between EBV and several histopathological features of the samples.

Results: EBV was detected in 39% of prostate cancer and 24% of BPH samples. The histopathological analysis of prostate cancer samples identified all samples as prostatic adenocarcinoma of acinar type, while statistical analyses revealed EBV-positive samples to exhibit significantly higher ($p<0.05$) Gleason major and total Gleason scores as compared to EBV-negative samples. In the EBV positive samples, variable expression patterns of latency-associated genes were observed, where most of the samples exhibited EBV latency II/III-like profiles in prostate cancer, while latency-II-like profiles in BPH samples.

Conclusion: This study suggests a high prevalence of EBV in prostate samples, where EBV exhibited latency II/III-like profiles. Furthermore, EBV-positive samples exhibited a higher Gleason score suggesting a possible link between EBV and onset/progression of prostate cancers. However, future functional studies are required to understand the role of the EBV gene expression profile in the onset/progression of prostate cancer.

Introduction

Globally, prostate cancer is the most frequently diagnosed cancer in men [1]. The pathophysiology of prostate cancer involves both genetic and acquired factors. Despite being extensively studied, several molecular events responsible for the *de novo* emergence and progression of neoplastic change in the prostate gland remain unclear [2]. Recent studies have shown an association between certain viral infections and the onset/progression of prostate carcinoma. The most common infections associated with prostate carcinoma are human papillomavirus (HPV), human herpesvirus type 8 (HHV8), Epstein-Barr virus (EBV), human herpes simplex virus type 2 (HHV2), etc. [3–5]. However, little is known about the molecular changes that these viral agents may induce in the prostate epithelial cells that might lead to the initiation or progression of prostate cancer. Some studies have demonstrated the ability of HHV8 to modulate JAK/STAT3, VEGF, and NF-κB pathways as well as downregulate androgen receptor expression to promote prostate cancer progression [3, 6].

Similar to HHV-8, EBV is a known human oncovirus, which has been labeled as Group I carcinogenic risk factor to humans based on causality for nasopharyngeal carcinoma, gastric carcinoma, Burkitt's lymphoma, non-Hodgkin's lymphoma (immunosuppression related), and Hodgkin's lymphoma [7]. EBV has predominantly been shown to maintain type II latency profiles in the nasopharyngeal carcinoma [8, 9], while in the EBV-associated gastric carcinoma and Burkitt's lymphoma, EBV predominantly maintains the latency I profile [10]. In immunosuppressive patients, however, who develop EBV-associated lymphomas tend to have a latency III profile. The expression of EBV latency-associated genes has been associated with invasion, cell proliferation, and anti-apoptosis [11].

EBV has been reported in prostate cancer epithelial cells [12–14]. However, there is a dearth of data exploring virological features, such as the latency profile that EBV maintains in prostate cancer samples or the relationship between EBV and histopathological features of cancer.

In this study, we attempted to fill this gap by performing PCR-based screening of prostate cancer samples to detect EBV, followed by the analysis of expression of EBV latency-associated genes to characterize the EBV latency stage profile in prostate carcinoma biopsy samples. Finally, we analyzed the relationship between EBV and several histopathological features of prostate cancer.

Materials & Methods

Sample collection

The sample size for this study was calculated considering the incidence of prostate cancer in Pakistan to be 5.3% per 100,000 people, with a marginal error, and a confidence interval of 5% and 95%, respectively [15, 16]. Using the above parameters, the sample size was calculated to be 73. However, we were able to procure a total of 99 FFPE tissue blocks from the years 2019 and 2020, with a confirmed diagnosis of prostate cancer. In addition, a total of 33 FFPE tissue blocks from the year 2020, with a confirmed diagnosis of benign prostatic hyperplasia (BPH) were also included. The samples/blocks were obtained from the Department of Pathology and Laboratory Medicine at the Aga Khan University (AKU), Karachi after obtaining informed consent from all subjects. The study was approved by the AKU Ethics Review Committee (AKU-ERC #: 2021-1460-18525). All methods were performed in accordance with the relevant guidelines and regulations.

Histopathological analysis of prostate cancer biopsy samples

The FFPE tissue blocks were used to prepare slides for hematoxylin and eosin staining using standard protocol [17]. The tumors were graded using the International Society of Urological Pathology (ISUP) 2014 / WHO 2016 prostate cancer grade group system [18]. The specimens were graded by documenting histopathological parameters, such as Gleason major, minor and total scores, perineural invasion, and infiltration of lymphocytes in the specimen. To characterize the presence of lymphocytes in the tissue, light microscopy was used and the presence of lymphocytes was categorized into zero, +1, +2, +3 for the presence of zero, 1-12, 13-21, and >22 lymphocytes respectively.

DNA extraction from prostate carcinoma and benign prostatic hyperplasia FFPE tissue blocks

For each given sample, four 10 µm thick FFPE sections were cut using a microtome and were stored at room temperature into two autoclaved 1.5 ml microcentrifuge tubes each for RNA and DNA extractions until further use. In the first step, the sample was deparaffinized. For this purpose, each sample was washed with 1000 µl of xylene and mixed by vortexing for 30 seconds, followed by incubation for 10 minutes on a shaker at room temperature. After incubation, the tubes were centrifuged at 15,000 rpm for 2 minutes, and subsequently, the xylene was removed. This step was repeated twice until all the paraffin was replaced by xylene. In the next step, xylene was removed from the tissues using 100% ethanol. For this purpose, 1.5 ml of 100% ethanol was added to each sample and mixed using vortex for 30 - 60 seconds. After this, the tubes were left on the shaker for 5 minutes and then centrifuged at 15,000 rpm for 2 minutes followed by removal of the liquid phase. This step was repeated twice until all the xylene was removed. Finally, the samples were gradually rehydrated using different concentrations of ethanol (95% and 70% respectively). For this purpose, 1.5 ml of 95% ethanol was added to the dehydrated samples and mixed using vortexing for 30 seconds, after which they were kept on a shaker for 10 minutes and then centrifuged at 15,000 rpm for 2 minutes. This step was repeated once using each concentration, and the final step was performed using deionized water. Finally, DNA was extracted from each sample using DNeasy® Blood & Tissue kit (Qiagen, USA), following the manufacturer's instructions. The DNA was stored at -80□C until further use.

Extraction of RNA by TRIzol-chloroform method and cDNA synthesis

RNA was extracted from the tissues using the TRIzol-chloroform method [19]. Briefly, following the tissue digestion, 700 µl of TRIzol® reagent, (Invitrogen, Thermo Fisher Scientific, Inc.) was added to each sample and the samples were allowed to incubate on ice for 5 minutes to allow the disassociation of nucleoprotein complexes. After the incubation, 200 µl of

chloroform was added to each tube, and contents were mixed vigorously, followed by another incubation at 4°C for 10 -15 minutes, and centrifugation for 5 minutes at 12,000 rpm, to allow the phase separation in the mixture. Following this centrifugation, the upper aqueous phase, where RNA is concentrated, was transferred to a fresh autoclaved 1.5 ml microcentrifuge tube without disturbing the interphase, and chilled 1000 µl isopropyl alcohol was added and incubated for 10 minutes at room temperature to chelate the RNA from the aqueous phase. Following the incubation, the tubes were centrifuged for 10 minutes at 12,000 rpm to obtain a white pellet of pure RNA at the bottom of the tube. The pellet was washed with 1000 µl of 70% ethanol and left to air dry. The pellet, containing RNA, was finally resuspended in 50 µl of nuclease-free water. The RNA was stored at -80°C until further use.

To remove the genomic DNA contamination in the RNA samples, and before cDNA synthesis, total RNA was treated with DNase I. For this purpose, 1 µg the total RNA template was combined in a 0.2 ml tube with 1 µl of (10X) reaction buffer containing $MgCl_2$, 1 µl of DNase-I, RNase-free 1U/1µl (Thermo Fisher Scientific, Cat. No. EN0521), and suitable volume of nuclease-free water for a final volume of up to 10µl. The prepared reaction was incubated for 30 minutes at 37°C in the Master cycler X50a (Eppendorf, Germany). To prevent the hydrolysis of RNA after the DNase-I treatment, 1µl of 50 mM EDTA was added and samples were allowed to incubate for 10 minutes at 65°C. The DNase-I treated total RNA, from the above step, was converted to cDNA using the OneScript® plus cDNA synthesis kit (ABM, Canada. Cat. No. G236) following manufacturer's instructions and stored at -20°C till further use.

Conventional PCR for the detection of EBV in prostate cancer and benign prostatic hyperplasia samples

To detect the presence of EBV in the prostate cancer samples (n= 99), conventional PCR was employed using the EBNA-2 gene primers, since EBNA-2 is constitutively expressed in EBV-infected cells [20]. For PCR reaction, 100-150 ng of DNA template was combined with the 4 µl of BesTaq™ master mix (2X) (ABM, Canada, Cat. no. G464), 1 pM of custom-made forward and reverse primers (Table 1) (Macrogen, USA) and nuclease-free water to a final volume of upto10µl. The above reaction was used in PCR with following cycling conditions: initial denaturation for 10 minutes at 95°C, followed by 36 cycles of denaturation for 15 seconds at 95°C, annealing for 1 minute at 60°C, and an extension for 30 seconds each at 72°C, followed by the final extension for 1 minute at 72°C. The amplicons from the reaction were analyzed on 1.8% agarose gel against a 50-bp ladder (Promega, USA) using ChemiDoc® imaging system (Bio-Rad Laboratories, USA). The amplicons showing bands at 96 bps were considered positive for EBNA-2.

Latency mapping of EBV in prostate cancer and benign prostatic hyperplasia tissue samples using quantitative Polymerase Chain Reaction (qPCR)

Following the identification of EBV-positive prostate cancer tissues, a quantitative real-time PCR was employed to analyze the expression of EBV latency-associated genes (*EBNA-3B, EBNA-3A, EBNA-2, EBNA-1, LMP-2A, LMP-2, LMP-1, EBER-2, EBER-1, BZLF-1, AND BHRF-1*) and determine the EBV-latency profile in prostate cancer samples. For this purpose, 2µl of cDNA sample was combined with a mixture containing 4 µl of BlasTaq™ (2X) qPCR master mix (ABM, Canada, Cat. No. G891), forward and reverse gene-specific primers (Table 1) (Macrogen, USA) and nuclease-free water to a final reaction volume of up to 10µl in a 0.2 ml tubes (Bio-Rad Laboratories, USA. Cat. No. TLS0851). The prepared reactions were subjected to the following thermal cycling conditions using Bio-Rad 1000 thermal cycler CFX96 (Bio-Rad laboratories, USA): initial denaturation for 10 minutes at 95°C, followed by 40 cycles for denaturation for 15 seconds at 95°C, annealing for 1 minute at 45°C, and a cyclic extension for 30 seconds at 72°C). A melt curve analysis was set up between 55°C to 95°C with an increment of 0.5°C every 5 seconds to plot the specificity of the products. Each sample was run in duplicates, while non-template controls were supplied with an additional 2µl of nuclease-free water instead of cDNA template.

Table 1
shows EBV latency-associated genes along with sequences of the forward and reverse primers.

Genes	Sequence (5′-3′)
EBNA-1	Fwd TACAGGACCTGGAAATGGCC
	Rev TCTTTGAGGTCCACTGCCG
EBNA-2	Fwd GCTTAGCCAGTAACCCAGCACT
	Rev TGCTTAGAAGGTTGTTGGCATG
EBNA-3A	Fwd CCCCTTAACTCAACCCATTAACC
	Rev CGGCCCCTCCATTGGT
EBNA-3B	Fwd TGCCGCTGCAAGAGAGG
	Rev AGGTCCGATTGCAACATGGA
LMP-1	Fwd CAGTCAGGCAAGCCTATGA
	Rev CTGGTTCCGGTGGAGATGA
LMP-2	Fwd GGTTCTCCTGATTTGCTCTTCGT
	Rev CGCGGAGGCTAGCAACA
LMP-2A	Fwd TCCCTAGAAATGGTGCCAATG
	Rev GAAGAGCCAGAAGCAGATGGA
EBER-1	Fwd TGCTAGGGAGGAGACGTGTGT
	Rev TGACCGAAGACGGCAGAAAG
EBER-2	Fwd AACGCTCAGTGCGGTGCTA
	Rev GAATCCTGACTTGCAAATGCTCTA
BZLF-1	Fwd AAATTTAAGAGATCCTCGTGTAAAACATC
	Rev CGCCTCCTGTTGAAGCAGAT
BHRF-1	Fwd GGCTTACCTCGGTTCCCTCTTA
	Rev TCCCGTATACACAGGGCTAACAGT
Fwd = Forward primer; Rev = Reverse primer.	

Analysis of differences in the histopathologic features of the EBV-positive and EBV-negative prostate carcinoma tissues

To compare the difference in the mean Gleason scores (major, minor, and total) between EBV-positive and EBV-negative prostate cancer samples, independent samples t-test was used. Similarly, the Pearson Chi-Square test was applied to determine the association of perineural invasion, intratumoral lymphocytes, stromal lymphocytes, and benign tissue lymphocytic infiltration with EBV status (positive or -negative), while the Spearman correlation test was applied to study the relationship between different histopathological parameters and EBV status. For all the statistical tests used in this study, a $p<0.05$ was considered statistically significant. IBM-SPSS version 23.0 was used to analyze the data.

Results

Detection of EBV in prostate cancer samples and correlation of histopathological parameters

In the first step, 99 retrospectively collected formalin-fixed paraffin-embedded prostate cancer tissue blocks were screened for the presence of EBV. The results showed 39.39% of the prostate cancer tissues to be positive for EBV.

The biopsy samples were further analyzed by a trained histopathologist, and the corresponding Gleason scores were assigned. All 99 samples were identified as prostatic adenocarcinoma of acinar type. Analysis of histopathological parameters in EBV-positive and -negative samples showed the Gleason major scores (4.12 ± 0.64 vs 3.84 ± 0.58) and total Gleason scores (8.24 ± 1.22 vs 7.75 ± 1.03) to be significantly higher ($p<0.05$) in EBV-positive and EBV-negative samples, respectively. These observations were further supported by Spearman's rho test, where a weak positive correlation (R-value: 0.206; $p = 0.041$*)* was observed between EBV positive status and Gleason major and total scores (Table 2). The association with additional histopathological features, such as prognostic grade group, perineural invasion, intratumoral lymphocytes, stromal lymphocytes were not significantly different between the EBV-positive and -negative samples (Figure 1). Notably, the infiltration of lymphocytes in benign tissue adjacent to the tumor tissue was found to be zero in 15.9% of EBV-negative and 3.8% of EBV-positive samples, while 1+ in 52.3% of EBV-negative and 76.9% of EBV-positive samples.

Table 2

Comparison of mean Gleason scores of EBV-positive and EBV-negative groups using independent samples t-test: The table shows the mean score comparison of Gleason major, Gleason minor, and total Gleason scores in between positive and negative samples. The histopathological analysis of tumor tissues was done as per the International Society of Urological Pathology (ISUP) 2014 later ratified by WHO 2016 as the prostate cancer grade group system.

Histopathological parameter(s)	EBV-positive & EBV-negative samples	N	Mean	SD	*p-value*
Gleason score major	Negative	66	3.84	0.58	*0.038**
	Positive	33	4.12	0.64	
Gleason score minor	Negative	66	3.90	0.62	*0.18*
	Positive	33	4.12	0.78	
Gleason score (total)	Negative	66	7.75	1.03	*0.042**
	Positive	33	8.24	1.22	
Prognostic grade group	Negative	63	3.68	1.35	*0.71*
	Positive	36	3.58	1.25	
*p<0.05 was considered significant using independent sample t-test					

Detection of EBV and Latency mapping in prostate cancer biopsies

Expression of EBV latency-associated genes was analyzed to determine the EBV latency profiles in the prostate cancer samples (Table 3). The analysis showed variable expression patterns of latency-associated genes in EBV positive samples, where most of the samples exhibited non-classical EBV latency II/III-like profiles (Table 3). The Ct values for each latency-associated gene are given in Supplementary Table 1.

Table 3

Characterization of EBV latency profile in EBV-positive prostate carcinoma tissues: The latency profile was mapped based on the expression of the following latency-associated genes: *EBNA-3B, EBNA-3A, EBNA-2, EBNA-1, LMP-2A, LMP-2, LMP-1, EBER-2, EBER-1, BZLF-1*, and *BHRF-1.* The + and – signs show the presence and absence of gene expression, respectively.

Sample ID	*EBNA-1*	*EBNA-2*	*EBNA-3A*	*EBNA-3B*	*LMP-1*	*LMP-2*	*LMP-2A*	*EBER-1*	*EBER-2*	*BHRF-1*	*BZLF-1*
Prostate_RNA_7	+	+	+	+	+	+	+	+	+	+	+
Prostate_RNA_12	+	+	+	+	+	+	+	+	+	+	+
Prostate_RNA_14	+	+	-	+	+	+	+	+	+	+	+
Prostate_RNA_16	+	+	-	+	+	+	+	+	-	-	-
Prostate_RNA_17	+	+	+	-	+	+	+	+	+	+	+
Prostate_RNA_19	+	+	-	-	-	+	-	+	-	-	-
Prostate_RNA_21	+	+	+	+	+	-	+	+	-	+	-
Prostate_RNA_22	+	+	-	-	-	-	+	+	-	-	+
Prostate_RNA_24	+	+	-	+	+	+	+	+	+	+	+
Prostate_RNA_27	+	+	+	+	+	+	+	+	+	+	+
Prostate_RNA_28	+	+	+	+	+	-	+	+	-	-	-
Prostate_RNA_34	+	+	+	+	+	-	+	+	+	+	-
Prostate_RNA_38	+	+	+	-	+	+	+	+	-	+	+
Prostate_RNA_40	+	+	-	-	+	-	+	+	+	+	+
Prostate_RNA_41	+	+	-	+	+	+	+	+	+	+	+
Prostate_RNA_42	-	+	-	+	+	+	+	+	+	+	+
Prostate_RNA_43	+	+	-	-	+	+	+	+	-	+	+
Prostate_RNA_51	+	+	-	+	+	-	+	+	+	-	+
Prostate_RNA_52	+	+	+	+	+	+	+	+	+	+	+
Prostate_RNA_53	+	+	-	+	+	+	+	+	+	+	+
Prostate_RNA_54	+	+	-	+	+	+	+	+	-	-	+
Prostate_RNA_59	+	+	-	-	+	-	+	+	-	-	+
Prostate_RNA_63	+	+	+	+	+	+	+	+	+	+	+
Prostate_RNA_64	+	+	-	+	+	+	+	+	-	-	+
Prostate_RNA_ 65	+	+	-	+	+	-	-	+	-	-	+
Prostate_RNA_66	+	+	-	-	+	-	+	-	+	-	+
Prostate_RNA_69	+	+	+	+	+	+	+	+	+	+	+
Prostate_RNA_72	+	+	-	-	+	-	+	+	-	+	+
Prostate_RNA_77	+	+	+	+	+	+	+	+	+	+	+
Prostate_RNA_79	+	+	+	+	+	-	+	+	+	-	+
Prostate_RNA_82	+	+	-	-	+	-	+	-	+	-	+

Sample ID	*EBNA-1*	*EBNA-2*	*EBNA-3A*	*EBNA-3B*	*LMP-1*	*LMP-2*	*LMP-2A*	*EBER-1*	*EBER-2*	*BHRF-1*	*BZLF-1*
Prostate_RNA_86	+	+	+	+	+	+	+	-	+	+	+
Prostate_RNA_89	+	+	+	+	+	+	+	+	+	+	+
Prostate_RNA_90	+	+	+	+	+	-	+	+	+	+	+
Prostate_RNA_99	+	+	-	+	+	+	+	+	+	-	+
Prostate_RNA_100	+	+	-	+	+	+	+	+	+	+	+
Prostate_RNA_102	+	-	+	-	+	+	+	+	+	+	+
Prostate_RNA_106	+	+	+	-	+	+	+	+	-	+	+
Prostate_RNA_109	+	-	-	-	+	-	-	+	-	+	+

Detection of EBV and Latency mapping in benign prostatic hyperplasia (BPH) biopsies

We found 24.24% (8 out of 33 of the samples) of BPH biopsy samples to be EBV-Positive. In the next step, we analyzed the expression of EBV latency-associated genes (Table 1) to determine the EBV latency profiles in the benign prostatic hyperplasia samples. The analysis showed variable expression patterns of latency-associated genes in EBV positive samples, where all of the samples except one, that exhibited a latency-III-like profile, exhibited a latency II-like profile (Table 4). The Ct values for each latency-associated gene are given in Supplementary Table 2.

Table 4

Characterization of EBV latency profile in EBV-positive BPH samples: The latency profile was mapped based on the expression of the following latency-associated genes: *EBNA-3B, EBNA-3A, EBNA-2, EBNA-1, LMP-2A, LMP-2, LMP-1, EBER-2, EBER-1, BZLF-1*, and *BHRF-1.* The + and – signs show the presence and absence of gene expression, respectively.

Sample ID	*EBNA-1*	*EBNA-2*	*EBNA-3A*	*EBNA-3B*	*LMP-1*	*LMP-2*	*LMP-2A*	*EBER-1*	*EBER-2*	*BHRF-1*	*BZLF-1*
BPH_03	+	+	-	-	+	+	+	+	+	-	+
BPH_05	+	+	-	-	+	+	+	+	+	-	+
BPH_14	+	+	-	-	+	+	+	+	+	-	+
BPH_16	+	+	+	+	-	+	+	+	+	+	+
BPH_20	+	+	-	-	+	+	+	+	+	-	+
BPH_21	+	+	-	-	+	+	+	+	+	+	+
BPH_23	+	+	-	-	+	+	+	+	+	-	+
BPH_28	+	+	-	-	+	+	+	+	+	-	+

Discussion

In this study, we have screened prostate cancer samples for the presence of EBV, followed by the characterization of the EBV latency profile in prostate carcinoma samples and analysis of histopathological parameters in EBV-positive and EBV-negative groups.

Of the prostatic adenocarcinoma of acinar subtype samples, 39.39% of the samples were EBV positive. Our study is consistent with earlier studies, where EBV was identified in 40% of prostate cancer tissues in Australian males based on *in situ* PCR technique [12], and 37% of prostatic adenocarcinoma samples in the US based on immunohistochemistry [21]. In an Iranian study, EBV was found to be present in 49.3% of the prostate cancer samples [22]. Although, studies have reported the detection of EBV in prostate specimens, however, the role of EBV in the onset and progression of prostate cancer remains a moot point. For instance, a Swedish study did not find a significant difference in EBV detection between prostate cancer and benign prostatic hyperplasia tissues [23]. Similarly, an Australian study found a comparable (40%) distribution of EBV in both prostate carcinoma samples as well as normal prostate tissue [12]. However, the scope of the above-mentioned studies has been limited to only detection of EBV in both prostate cancer and normal prostate tissues, and none of them have undertaken the analysis of latency profiling of EBV in the prostate cancer samples.

The screening of the BPH samples showed the presence of EBV in 24.24% of the samples, where EBV predominantly exhibited a type II-like latency profile. Our reported EBV positivity percentage in BPH samples is higher than all previously reported studies. For example, a Swedish study reported 8.8% benign prostatic hyperplasia samples to be EBV-positive based on PCR-based detection of EBV [23]. An Iraqi study found an EBV-positive percentage of 10% in BPH samples based on immunohistochemical analysis of EBV-EBER proteins [24]. Another Iraqi study reported 5% and 25% of EBV-positive status in benign prostatic hyperplasia samples and prostate carcinoma, respectively [25]. Further studies need to be carried out to establish the difference between EBV infection and latency in benign prostatic hyperplasia and prostate adenocarcinoma.

In EBV-positive epithelial cancers, the expression of EBV latency genes has been reported to be found in almost all cancerous cells [26], thereby, showing a strong association between EBV and EBV-positive epithelial cancers. Our findings show that EBV exhibits non-classical EBV latency II/III-like profiles in adenocarcinoma of prostate cancer based on the expression of *EBNA-3B, EBNA-3A, EBNA-2, EBNA-1, LMP-2A, LMP-2, LMP-1, EBER-2, EBER-1, BZLF-1*, and *BHRF-1* (Table 3). EBV infection with subsequent expression of EBV latency genes products might enhance survival of premalignant cells along with the conferred antiapoptotic properties to epithelial cells which are in the premalignant state, thereby, increasing the chances of harboring genetic alteration or mutations [27]. At the same time, the genetic changes, such as inflammation in stromal portions of tissues, may further result in modulation of EBV latency gene expression which may alter growth properties of the tissue and might preselect and pave the pathway towards carcinogenesis [28]. These findings are comparable to earlier reports that have shown that EBV maintains a type II latency profile in EBV-associated epithelial cancers, such as EBV-associated gastric carcinoma (EBVaGC) and nasopharyngeal carcinoma [27]. Recent studies have reported that LMP2A and LMP1 play a role in epithelial-to-mesenchymal transition in nasopharyngeal carcinoma, thereby, playing a critical role in the onset of cancer [29].

Histopathological analysis of EBV-positive and -negative tissues showed a significant difference in EBV-positive and EBV-negative prostate adenocarcinoma samples, where EBV-positive samples exhibited a higher Gleason score when the comparison of means of Gleason scores was made in between two groups (Table 2). Tumor grading based on the Gleason score is a strong predictor of the prognosis, and higher Gleason scores are associated with a worse prognosis [30]. Some reports have shown that mutations of the *p53* gene which were probably mediated by BKV viral infection in prostate cancer are found to be associated with advanced tumor stage with high Gleason scores [31], but none is reported to show the association of EBV-positive status of prostate carcinoma with the Gleason scores. Another study found a significant association between HPV infection in prostate carcinoma and corresponding high Gleason scores [32]. However, further studies are required to understand the putative mechanisms by which EBV infection in prostate carcinoma may have an association with the tumor grade and the prognosis.

In summary, the presence of EBV in prostate cancer tissues, maintenance of type II/III profiles, and association with high Gleason score might suggest a link between EBV infection and initiation and/or promotion of prostate cancer. However, further studies are required to fully understand the how gene expression profile of EBV contributes to prostate cancer progression.

Declarations

Acknowledgment:

The study was funded by the Pakistan Higher Education commission grant 8722/Sindh/ NRPU/R&D/HEC/ 2017.

Conflict of interest:

None to declare

Author's contribution:

Conceptualization: SHA, FA; Methodology: KA, AS, SF, GH, KG; First draft: KA, AS; Final draft and review: KG, NM, SHA; Supervision: SHA

Data availability:

All data generated or analyzed during this study are included in this published article (and its supplementary information files).

References

1. Sung, H., et al., *Global cancer statistics 2020: GLOBOCAN estimates of incidence and mortality worldwide for 36 cancers in 185 countries.* CA: a cancer journal for clinicians, 2021. **71**(3): p. 209-249.
2. Beg, S., F. Khani, and B.D. Robinson, *Pathology of Prostate Cancer*, in *Precision Molecular Pathology of Prostate Cancer*. 2018, Springer. p. 37-56.
3. Mygatt, J.G., et al., *Oncogenic herpesvirus HHV-8 promotes androgen-independent prostate cancer growth.* Cancer research, 2013. **73**(18): p. 5695-5708.
4. Luo, J., et al., *Fusion genes associated with progressive prostate cancer*. 2019, Google Patents.
5. Banerjee, S., et al., *Microbiome signatures in prostate cancer.* Carcinogenesis, 2019. **40**(6): p. 749-764.
6. Abidi, S.H., et al., *Viral etiology of prostate cancer: genetic alterations and immune response. A literature review.* International Journal of Surgery, 2018. **52**: p. 136-140.
7. Wong, Y., et al., *Estimating the global burden of Epstein–Barr virus-related cancers.* Journal of Cancer Research and Clinical Oncology, 2021: p. 1-16.
8. Hu, L., et al., *Comprehensive profiling of EBV gene expression in nasopharyngeal carcinoma through paired-end transcriptome sequencing.* Frontiers of medicine, 2016. **10**(1): p. 61-75.
9. Hau, P.M., et al., *Targeting Epstein-Barr virus in nasopharyngeal carcinoma.* Frontiers in Oncology, 2020. **10**: p. 600.
10. Yang, J., et al., *Epstein–Barr virus-associated gastric cancer: A distinct subtype.* Cancer Letters, 2020. **495**: p. 191-199.
11. Ayee, R., et al., *Epstein Barr virus associated lymphomas and epithelia cancers in humans.* Journal of Cancer, 2020. **11**(7): p. 1737.
12. Whitaker, N.J., et al., *Human papillomavirus and Epstein Barr virus in prostate cancer: Koilocytes indicate potential oncogenic influences of human papillomavirus in prostate cancer.* The Prostate, 2013. **73**(3): p. 236-241.
13. Nahand, J.S., et al., *Possible role of HPV/EBV coinfection in anoikis resistance and development in prostate cancer.* BMC cancer, 2021. **21**(1): p. 1-19.
14. Chen, Y. and J. Wei, *Identification of pathogen signatures in prostate cancer using RNA-seq.* PLoS One, 2015. **10**(6): p. e0128955.
15. *Sample Size Calculator* 2021 20 November 2021]; Available from: https://www.calculator.net/sample-size-calculator.html.

16. Idrees, R., et al., *Cancer prevalence in Pakistan: meta-analysis of various published studies to determine variation in cancer figures resulting from marked population heterogeneity in different parts of the country.* World J Surg Oncol, 2018. **16**(1): p. 129.
17. Feldman, A.T. and D. Wolfe, *Tissue processing and hematoxylin and eosin staining*, in *Histopathology*. 2014, Springer. p. 31-43.
18. Humphrey, P.A., et al., *The 2016 WHO Classification of Tumours of the Urinary System and Male Genital Organs-Part B: Prostate and Bladder Tumours.* Eur Urol, 2016. **70**(1): p. 106-119.
19. Chomczynski, P. and K. Mackey, *Short technical reports. Modification of the TRI reagent procedure for isolation of RNA from polysaccharide- and proteoglycan-rich sources.* Biotechniques, 1995. **19**(6): p. 942-5.
20. Pich, D., et al., *First days in the life of naive human B lymphocytes infected with Epstein-Barr virus.* MBio, 2019. **10**(5): p. e01723-19.
21. Grinstein, S., et al., *Demonstration of Epstein-Barr virus in carcinomas of various sites.* Cancer research, 2002. **62**(17): p. 4876-4878.
22. Nahand, J.S., et al., *Anoikis Resistance and Development in Prostate Cancer: The Possible Role of HPV/EBV Coinfection.* 2021.
23. Bergh, J., et al., *No link between viral findings in the prostate and subsequent cancer development.* British journal of cancer, 2007. **96**(1): p. 137-139.
24. Ali, S.H.M. and S.H.M. Al-Alwany, *Molecular localization of Epstein Barr virus and Rb tumor suppressor gene expression in tissues from prostatic adenocarcinoma and benign prostatic hyperplasia.* Iraqi journal of biotechnology, 2014. **13**(2).
25. Mezher, M.N. and A.A.H. Auda, *Relationship of Human Papilloma Virus (HPV) and Epstein Barr Virus (EBV) with Prostate Cancer in AL-Najaf Governorate.* Research Journal of Pharmacy and Technology, 2017. **10**(10): p. 3283-3288.
26. Weiss, L.M. and Y.-Y. Chen, *EBER in situ hybridization for Epstein–Barr virus*, in *Hematological Malignancies*. 2013, Springer. p. 223-230.
27. Tsao, S.W., C.M. Tsang, and K.W. Lo, *Epstein–Barr virus infection and nasopharyngeal carcinoma.* Philosophical Transactions of the Royal Society B: Biological Sciences, 2017. **372**(1732): p. 20160270.
28. Naseem, M., et al., *Outlooks on Epstein-Barr virus associated gastric cancer.* Cancer treatment reviews, 2018. **66**: p. 15-22.
29. Zhu, N., et al., *EBV latent membrane proteins promote hybrid epithelial-mesenchymal and extreme mesenchymal states of nasopharyngeal carcinoma cells for tumorigenicity.* PLoS Pathogens, 2021. **17**(8): p. e1009873.
30. Yeong, J., et al., *Gleason grade grouping of prostate cancer is of prognostic value in Asian men.* Journal of clinical pathology, 2017. **70**(9): p. 745-753.
31. Russo, G., et al., *p53 gene mutational rate, Gleason score, and BK virus infection in prostate adenocarcinoma: Is there a correlation?* Journal of medical virology, 2008. **80**(12): p. 2100-2107.
32. Singh, N., et al., *Implication of high risk Human papillomavirus HR-HPV infection in prostate cancer in Indian population-A pioneering case-control analysis.* Scientific reports, 2015. **5**(1): p. 1-4.

Figures

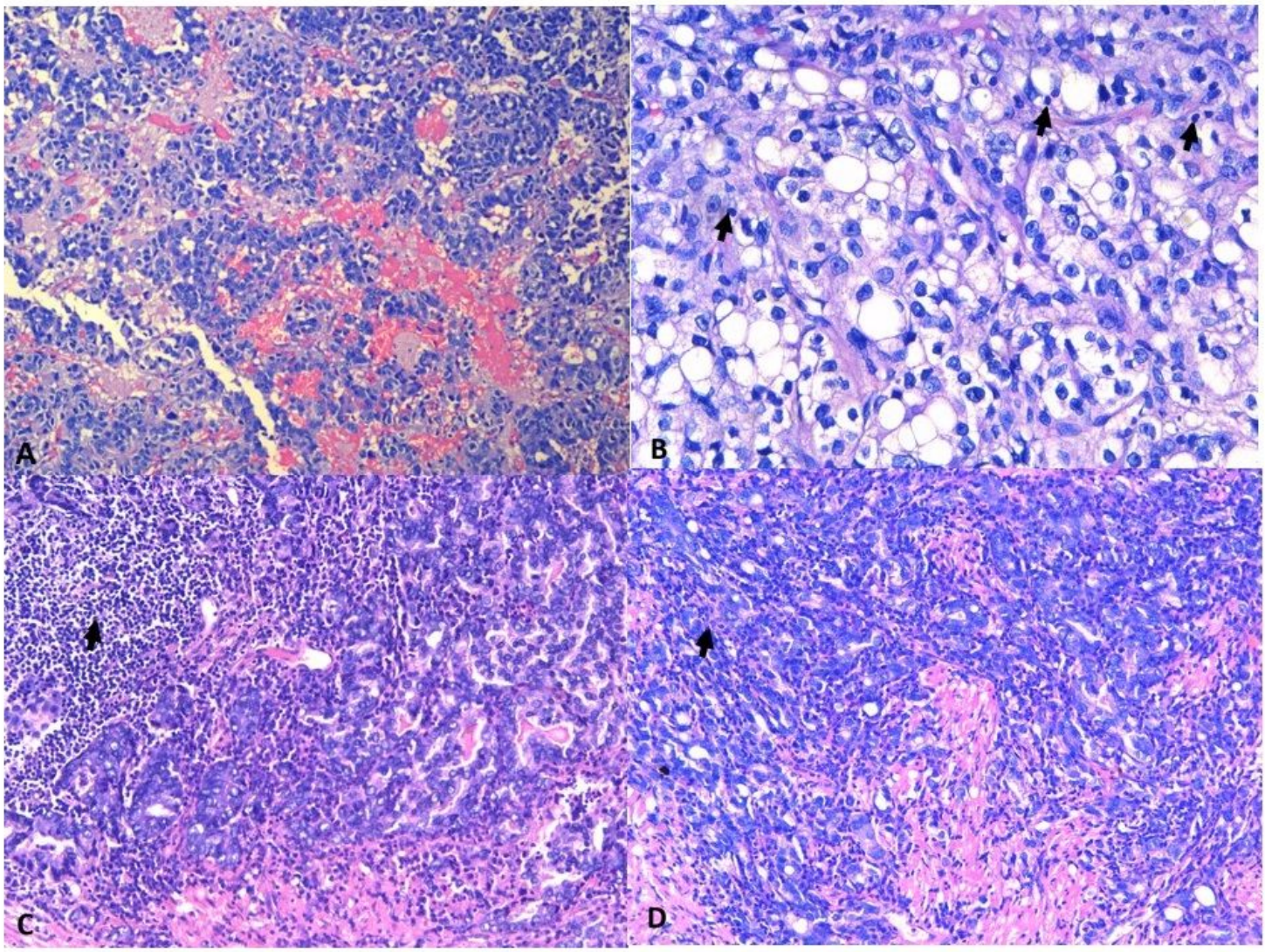

Figure 1

Representative histopathological images of EBV-positive and EBV-negative prostate cancer tissues: A-B) the histopathological images of EBV positive prostate adenocarcinoma of acinar type, Gleason score of 9 (4+5), with a prognostic grade of 5 (Hematoxylin and Eosin; original magnification: 100X). **B)** intratumoral lymphocytes (ITL) infiltration in the tumor marked with black arrows (H & E; 400X). **C-D)** the histopathological images of EBV-negative prostate adenocarcinoma of acinar type, Gleason score of 9 (4+5), with a prognostic grade of 5. **C)** Shows stromal lymphocytic infiltration (black arrows arrow) (Hematoxylin and Eosin; original magnification: 200X) **D**) the intratumoral lymphocytic infiltration. (Hematoxylin and Eosin; original magnification: 200X)

Supplementary Files

This is a list of supplementary files associated with this preprint. Click to download.

- SupplementTables.docx